 doi:10.20944/preprints202012.0286.v1

Article

High-Frequency Modeling and Filter Design for PWM Drives with Long Cables

Lei Wang [1], Yifan Zhang [2], Muhammad Saqib Ali [1], Guozhu Chen [1], Josep M. Guerrero [3]*, and Juan C. Vasquez[3]

[1] Department of Electrical Engineering, Zhejiang University, Hangzhou, China; leiwang_ee@zju.edu.cn
[2] Polytechnic Institute, Zhejiang University, Hangzhou, China; 21760552@zju.edu.cn
[3] Center for Research on Microgrids (CROM), Department of Energy Technology, Aalborg University, 9220 Aalborg, Denmark joz@et.aau.dk
* Author to whom correspondence should be addressed.

Abstract: Aiming for the problems emerging in the PWM drive system with long cables, accurate modeling of power cables is the premise to predict and analyze the relevant phenomenon, and a proper filter design is the key solution to these problems. This paper proposes high-frequency cable models to represent the frequency-dependent characteristics, especially for the high-frequency resistance of the cable that is an easily overlooked factor but determines the damping of overvoltage. The proposed models can be used for accurately representing the cable parameters in a wide frequency range, and correctly simulating the differential mode (DM) overvoltage and common mode (CM) current, including the peak value, oscillation frequency and damping of the transient waveform. In addition, improved filter networks are proposed to suppress the DM voltage and CM current, with the merit of low losses, small volume and an excellent ability of suppressing overvoltage. The proposed cable models and the filter design have been validated in a 750W PWM drive system with 200m power cables.

Keywords: cable modeling; motor drives; filter design; DM overvoltage; CM current; PWM

1. Introduction

The Pulse Width Modulated Voltage Source Inverter (PWM-VSI) plays an important role in the Adjustable Speed Drive (ASD) system, leading to a more effective drive application. New power semiconductor devices with high switching speed improve the power density of ASD application [1], but electromagnetic interference (EMI) issues related with high frequency have emerged. The high-frequency problems will be more serious if long power cables require to be connected between the inverter and motor, like the ASD in offshore or land-based well [2], mining plants [3] and wind farm [4], because the voltage reflection owing to cable-motor impedance mismatch occurs along the cable and twice or higher the dc-bus voltage appears at the motor terminal, which may destroy the insulation of cables and motors. In addition, high dv/dt applied on the parasitic capacitance of cable will produce high-frequency current, possibly resulting in the malfunction of the drive system. Apart from the insulation problem of motors, the generation of bearing current caused by high dv/dt will shorten the motor lifetime [5]. To investigate and solve the problems of EMI and overvoltage, accurate modeling of the drive system and an elaborated filter design are the research objective.

Among the modeling of the long-cable drive system, the cable model is the most crucial part, which should be consistent with the practical high-frequency response. Certainly, researchers have also studied at full steam trying to establish accurate models for the inverter and motor, which are the other two parts of a simplified drive system. The inverter is often regarded as a voltage source with trapezoidal or parabolic shape, and internal impedance may be considered sometimes. Various high-frequency models have been suggested for the motor [6-10], to represent the high-frequency characteristic of motors. Charactering each phase of motors with a single circuit [6-8] is a universal high-frequency model when the motor windings of every phase are symmetrical and balanced.

 doi:10.20944/preprints202012.0286.v1

Besides, the rational function is used to fit the measured motor parameters [9], and [10] proposes a motor model for both time domain and frequency domain. As for cable models, it's known that the low frequency model is not adequate to analyze the high-frequency phenomenon occurring in the drive system with long cables. [11], [12] apply mathematical models on fitting the cable parameters dependency with frequency, but it is rather abstract of the mathematical derivation. Cable modeling in frequency domain is another way worth exploring [16], which has both the advantage of short simulation time and the disadvantage of difficulty in constructing the inverter or harmonic voltage source. The lumped-parameter model has been widely adopted, including the multi-order per section [13], [14], the second-order section [15], if classified by the section orders of model. Although the model based on the time domain characteristics is widely accepted, the modeling process of multi-order model with rather higher accuracy is a little complicated. Generally, it's hard to find a modeling method including both simplicity and accuracy simultaneously. In addition, researchers almost only pursuit the accuracy of cable impedance but neglect the resistance which is a minor part of high-frequency impedance but plays an important role in simulating high-frequency phenomenon, leading to the inaccuracy in simulating the overvoltage and CM current.

The passive filter is an effective method to solve the high-frequency problems in the long-cable drive system, which is easier to be realized compared with insulation enhancement of motors or modulation improvement of inverter control. The conventional LR, RLC and RC filters are widely used as differential mode (DM) filter [17-19], and their parameters calculation is summarized in [19]. However, there are resistors in those filters as impedance matching components and power-consuming components as well, contributing to the low efficiency when used in the low-power drive system. At the same time, common mode (CM) noise should also be suppressed with the corresponding CM filter, and it can be integrated as one filter with the DM filter in [20], which is hard to be designed and manufactured. [21] proposes an innovative CM transformer whose magnetic core is smaller than that of the conventional CM choke, which has been adopted in this paper.

In this paper, the two high-frequency cable models are proposed to improve the frequency-dependent characteristics of power cable, and then both models have been compared, showing the proposed ladder circuit has similar and even better performances but takes more time to calculate and simulate. After the evaluation of the proposed model parameters with analytical design equations provided, the entire cable model has been constructed, whose validity and effectiveness have been verified through the practical 200m power cables. In order to check the simulation results of DM overvoltage and CM current based on the model of the drive system including long cables, inverter and motor model, the experiment has been carried out on a 750W test platform. Apart from the comparation between simulation results of the proposed model and experimental results, other cable models available in some software program are also embodied. Finally, the new filter networks, especially for the small hp motor with a strict working voltage requirement and long leads, are proposed to suppress the DM overvoltage and CM current. The advantages of proposed filter network including volume, efficiency and suppressing ability of overvoltage have also been confirmed by the experiment on the same test platform.

2. High-Frequency Modeling for the Power Cables

Accurate modeling for the power cables plays the most important role in predicting overvoltage and spike current and optimizing the filter design. It's known that the distributed-parameter model is normally used to represent the characteristics of cable, derived from the differential equation of transmission line, but it does not include the frequency-dependent nature of the cable parameters, especially in the high-frequency range. On the contrary, the lumped-parameter circuit, with the merit of flexibility, and relatively easy realization, could provide such frequency-dependent characteristic once the lumped segment is accurate and its amount is adequate. Certainly, the most basic and conventional PI model, shown in Figure 1(a), as one of the lumped-parameter circuits, is not enough to display frequency-dependent characteristic but serves as the basis of most improved distributed-parameter models, comprised with series and parallel branches.

Preprints (www.preprints.org) | NOT PEER-REVIEWED | Posted: 11 December 2020 doi:10.20944/preprints202012.0286.v1

The frequency-dependent phenomenon is mainly caused by dielectric losses, skin and proximity effects appearing in the high-frequency range, resulting the variation of cable parameters with frequency. In detail, the series inductance and parallel capacitance only have a slight decrease as frequency increases [17], showing inverse correlation with frequency, but the series resistance instead increases sharply and nonlinearly as frequency increases. There is a similar phenomenon existing in the parallel resistance, which makes small contribution to the cable characteristic because of its enormous value of resistance. For the convenience of representing these high-frequency characteristics, impedance performance of cable is usually selected as the evaluation index that actually only represents a part of cable characteristics, but researchers pay much attention to the improved models to make the fitted impedance superimpose well the measured ones [19][22]. When the frequency increases, the inductance will dominate the impedance, at the same time the resistance changes fast but it's much smaller than inductance, resulting in the enormous fitting deviation of high-frequency resistance, with a good agreement of impedance performance though. In other words, the good agreement between fitting and measured impedance only indicates that the inductance or capacitance of model is consistent with the that of cable in high-frequency range, without considering the consistence of series and parallel resistance of high frequency.

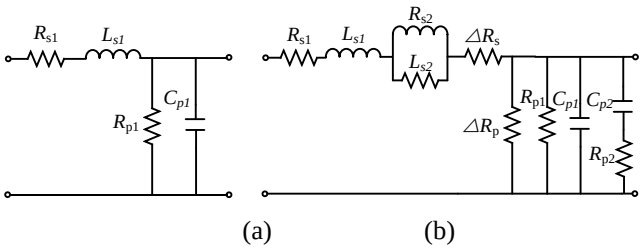

Figure 1. Elementary cell of the cable model

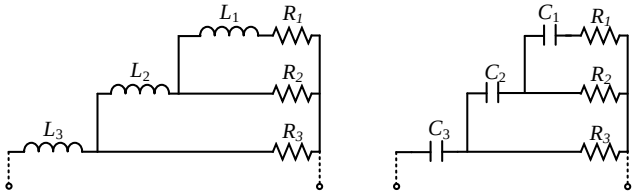

Figure 2. Elementary cell of the ladder network: (a) R-L ladder, (b) R-C ladder

To fit the practical high-frequency characteristics of cable series resistance as well as inductance, the R-L ladder circuit is introduced shown in Figure 2(a), consisting of R and L elements that are independent with frequency as a single element but contribute to the frequency-dependent characteristics of cable series resistance and inductance as a whole, and it's similar for parallel resistance and capacitance to introduce the R-C ladder circuit. The more branches of the ladder network, the higher the fitting accuracy apparently, but the more complicated the parameters calculation and the model simulation. As a matter of a fact, the parameters calculation of ladder network with even only three or four branches is still not easy, since it includes complex number and many variables, though some mathematical simplifications could be conducted in the calculation process [13]. The three and four branches R-L ladder networks, with parameters derived from corresponding sets of impedance known at different frequency points in Table 1 and Table 2, are constructed to fit the curve of series resistance versus frequency, shown in Figure 3, and the simulation results of both ladders are in rather good agreement. Better fitting performance of inductance has been realized that is not shown here, because the variation of inductance with frequency is not very distinct and rather easier to be fitted, and so does admittance, which will all be discussed afterwards. However, there should be a trade-off between the accuracy of fitting series and parallel resistance and cost of modeling. It's known that the cable parameters should be evaluated over the frequency spectrum of voltage pulse, from several hundreds of hertz to several megahertz, but the overvoltage at the motor terminal rings at the same frequency as the natural frequency of the cable, decided by the cable length and its intrinsic

Preprints (www.preprints.org) | NOT PEER-REVIEWED | Posted: 11 December 2020 doi:10.20944/preprints202012.0286.v1

characteristics. The natural frequency (f_R) of the cable is a function of cable inductance per unit length (L_0), cable capacitance per unit length (C_0) and cable length (l), further defined using cable length and relative permittivity (ε_r) , and it can be expressed as:

$$f_R = \frac{1}{4l\sqrt{L_0 C_0}} = \frac{c}{4l\sqrt{\varepsilon_r}} \tag{1}$$

The cable resistance at the oscillation frequency, almost fixed for specific cable from (1), plays an important role in the overvoltage simulation, which determines the decay speed or damping of overvoltage. In addition, although the ladder network fits the characteristics of cable well, it takes much efforts to construct and still can't guarantee the high accuracy of cable series and parallel resistance at the oscillation frequency. It can't be denied that the ladder circuit with more branches is an effective model, if the simulation and calculation time are not taken into consideration. Therefore, on the other side, the requirements of cable modeling can be changed as the consistence of inductance and capacitance in whole frequency range, but resistance consistence at natural frequency (f_R) and some resistance inconsistence permitting at other frequency. Then, an improved model (Figure 1(b)) is proposed based on basic PI cable model, in which parallel branch (R_{p2}-C_{p2}) represents the dielectric loss and fits the capacitance and parallel resistance characteristics varying with frequency; series branch (R_{s2}-L_{s2}) denotes the skin and proximity effects, and fits the inductance and series resistance characteristics varying with frequency; supplement branch ΔR_s-ΔR_P) is used for the modification of series and parallel resistance at cable resonance frequency. Besides, the proposed model is available in both DM and CM equivalent circuit only with parameters differences. In a typical inverter-fed motor drive, there are two phases in parallel and other phase in return between the inverter and motor, as the DM equivalent circuit of cable, modelled to simulate the overvoltage phenomenon at the motor side. As for CM equivalent circuit, it consists of three phase lines in parallel and ground line as returning cable, used to analyze the CM noise of long cable system. In case of disambiguation of the following

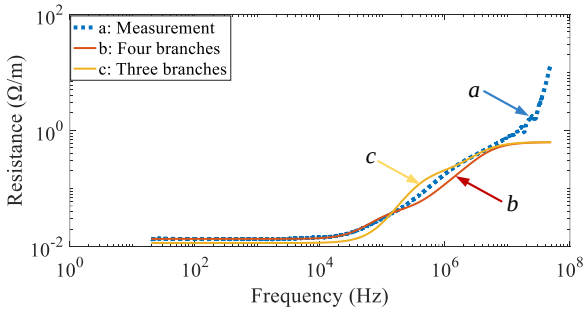

Figure 3. Per unit cable resistance of the measurement and simulation

Table 1. Measured points for three branches

Frequency (Hz)	Impedance (Ω)	Angle (º)
28710	0.0698	80.71
1.78M	3.7289	87.19
5.01M	10.2518	88.13

Table 2. Measured points for four branches

Frequency (Hz)	Impedance (Ω)	Angle (º)
28710	0.0698	80.71
167k	0.3802	85.83
1.78M	3.7289	87.19
5.01M	10.2518	88.13

Preprints (www.preprints.org) | NOT PEER-REVIEWED | Posted: 11 December 2020 doi:10.20944/preprints202012.0286.v1

sections, the proposed model means the cable model in Figure 1(b) rather than the ladder network in Figure 2.

3. Parameters Evaluation of the Proposed Cable Model

3.1. Parameters Calculation

The parameters of the proposed model could be determined by the short circuit (SC) and open circuit (OC) impedance of the power cables, which could be evaluated by impedance analyzer. For the purpose of getting exact cable parameters, the length of the test cable is critical for the impedance measurement, of which there should be no resonance in its impedance characteristic, meaning the cable should be short enough but the measurement of short cables could be affected by the instrument intrinsic deviation or the fixture impedance. Therefore, it's better to find the long cable with no resonance in the test frequency range. For convenience, the natural frequency of the cable could be roughly regarded as the first resonance frequency of cable impedance, then if the maximum measurement frequency is fmax, the length of the test cable (l_{test}) can be determined as:

$$l_{test} \le \frac{1}{4 f_{\max} \sqrt{L_0 C_0}} = \frac{c}{4 f_{\max} \sqrt{\varepsilon_r}} \tag{2}$$

The power cable used here is an unshielded, waterproof, PVC-insulated, four-core cable with 2mm-diameter conductor. The relative permittivity (ε_r) of the power cable is 3.85, so the maximum length of test cable is 1.27m. In fact, it's still not accurate to estimate the cable parameters at the region where the impedance curve is near the resonance point, thus the test cable selected here is 0.67m to leave enough margin, and its SC impedance curves in DM is shown in Figure 4. From the impedance curve, the inductance dominates the impedance after certain frequency where the impedance of cable inductor is much larger than cable resistance and the cable impedance curve is almost superimposed with the 20 dB/decade asymptote. At the same time, although the inductance varies with the frequency, the changing is not much significant like the cable resistance. As a result, combined with the proposed model and the SC equivalent circuit in DM (Figure 5), two sets of impedance points located in low frequency and high frequency are enough to evaluate the model inductance parameters (L_{s1}, L_{s2}), whereas only a part of the model resistance parameters (R_{s1}, R_{s2}) can be solved using the identical sets of points and extra DC resistance ($R_{SC\text{-}DC}$) of cable, with supplement resistance parameter (ΔR_s) calculated by the additional point located at the natural frequency (f_R) of the cable impedance. In general, series branch parameters of cable DM model could be determined by DC resistance of cable and three sets of points of cable impedance, including the low frequency impedance ($|Z_{SC\text{-}LF}|$, $\theta_{SC\text{-}LF}$, f_{LF}), the high-frequency impedance ($|Z_{SC\text{-}HF}|$, $\theta_{SC\text{-}HF}$, f_{HF}) and the natural frequency impedance ($|Z_{SC\text{-}Na}|$, $\theta_{SC\text{-}Na}$, f_{Na}), and their relationships are shown below:

$$L_{s1} + L_{s2} = \left|Z_{SC-LF}\right| \left[2\pi f_{LF}\right]^{-1} \tag{3}$$

$$L_{s1} = \left|Z_{SC-HF}\right| \left[2\pi f_{HF}\right]^{-1} \tag{4}$$

$$R_{s1} = R_{SC-DC} \tag{5}$$

$$R_{s1} + R_{s2} = \left|Z_{SC-HF}\right| \cos\theta_{SC-HF} \tag{6}$$

$$\Delta R_s = \left|Z_{SC-Na}\right| \cos\theta_{SC-Na} - Real\left[R_{s1} + j2\pi f_{Na} L_{s1} + R_{s2} \,//\, (j2\pi f_{Na} L_{s2})\right] \tag{7}$$

It is noted that the frequency at the low frequency region should be larger than the frequency point where the slope is changing from 0 to 20dB/decade, rather than the 0db/decade region of impedance curve. Similarly, the corresponding parallel parameters of cable in DM can be determined from the OC impedance curve of 0.67-meter cable section, as shown:

Preprints (www.preprints.org) | NOT PEER-REVIEWED | Posted: 11 December 2020 doi:10.20944/preprints202012.0286.v1

$$C_{p1}+C_{p2}=\left[\left|Z_{OC-LF}\right|(2\pi f_{LF})\right]^{-1} \tag{8}$$

$$C_{p1}=\left[\left|Z_{OC-HF}\right|(2\pi f_{HF})\right]^{-1} \tag{9}$$

$$R_{p1}=R_{OC-DC} \tag{10}$$

$$R_{p1}//R_{p2}=\left|Z_{OC-HF}\right|\left[\cos(-\theta_{OC-HF})\right]^{-1} \tag{11}$$

$$(\Delta R_p)^{-1}=Real(\left|Z_{Na}\right|\angle\theta_{OC-Na})^{-1}-Real\left[(R_{p1})^{-1}+j2\pi f_{Na}C_{p1}+(R_{p2}+(j2\pi f_{Na}C_{p2})^{-1})^{-1}\right] \tag{12}$$

All the cable parameters of DM model that have been calculated based on the 0.67m test cable could be transferred to per-unit parameters (Table 3), then a per-unit DM model will be constructed, which is more convenient to be used to build the long cable model. Similarly, the per-unit CM model could be established according to the same procedure using its corresponding measured results of SC and OC test. In addition, the proposed model should be applied to the symmetrical cable, or a little asymmetric cable depending on the degree of difference among impedance curves of different phases.

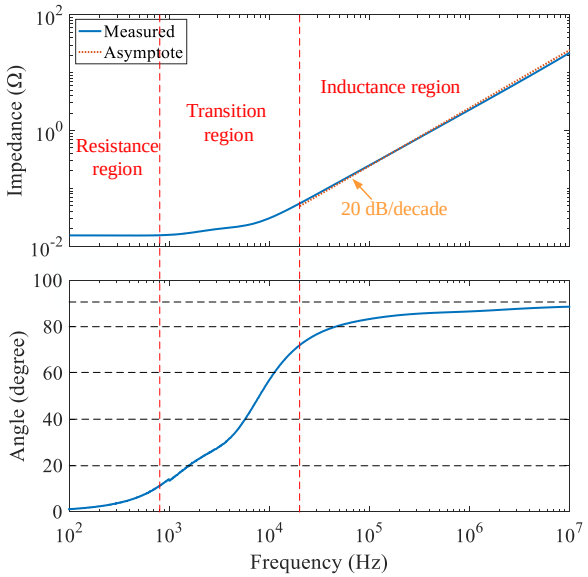

Figure 4. SC impedance of 0.67m cable in DM

Table 3. Per-unit parameters of the proposed model

Parameters	DM	CM
R_{s1}	13.5mΩ/m	15.1mΩ/m
R_{s2}	852.7mΩ/m	916.4mΩ/m
ΔR_s	38.8mΩ/m	22.8mΩ/m
R_{p1}	17.6MΩ/m	15.9MΩ/m
R_{p2}	6.4kΩ/m	8.0kΩ/m
ΔR_p	897.5kΩ/m	840.38kΩ/m
L_{s1}	522.3nH/m	432.8nH/m
L_{s2}	63.3nH/m	58.0nH/m
C_{p1}	86.5pF/m	104.5pF/m
C_{p2}	6.8pF/m	6.4pF/m

Preprints (www.preprints.org) | NOT PEER-REVIEWED | Posted: 11 December 2020 doi:10.20944/preprints202012.0286.v1

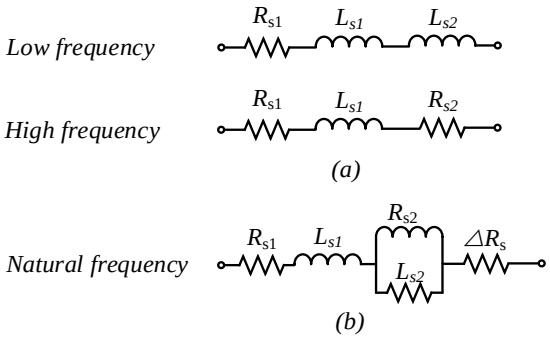

Figure 5. SC equivalent circuit at different frequency in DM

3.2. Impedance Verification

Although it has been discussed that the cable resistance of the proposed model at the oscillation frequency is same with the actual cable, the impedance characteristics in high-frequency region should been verified, which closely related with cable inductance and capacitance.

Since the proposed model is lumped-parameter model, whose performance is intimately related to the length represented by lumped cell, it's more accurate to use more cells to build the entire long cable model but it takes a long simulation time. The critical length of lumped segment depends on the rise time (t_r) of the PWM pulse from inverter, because the length of lumped segment should be much smaller than the wavelength of electromagnetic wave propagating on the cable (λ), which can be determined by:

$$f_p = \frac{1}{\pi t_r} \tag{13}$$

$$\lambda = \frac{c}{\sqrt{\varepsilon_r}} / f_p \tag{14}$$

In (13), f_P denotes the highest-frequency components of a PWM pulse derived from flourier analysis. To calculate the critical length of the test cable here, the ratio of the length of segment to the wavelength of electromagnetic wave is selected as 1.3×10^{-2}, then the critical length of the test cable is approximately 1 meter, with 160ns rise time of switching devices.

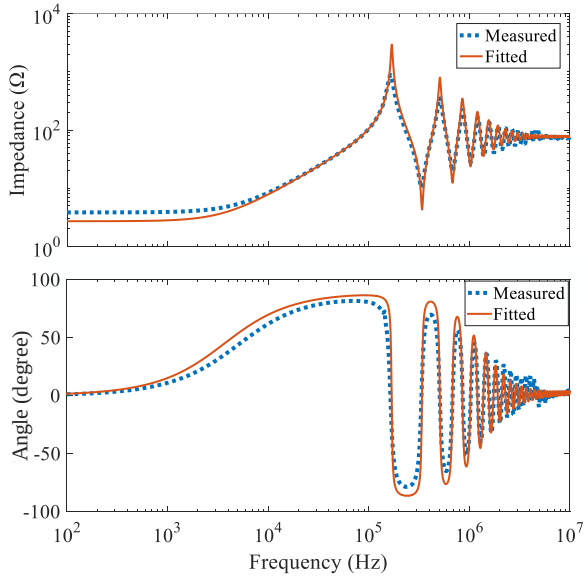

Figure 6. SC impedance of 200m power cable in DM

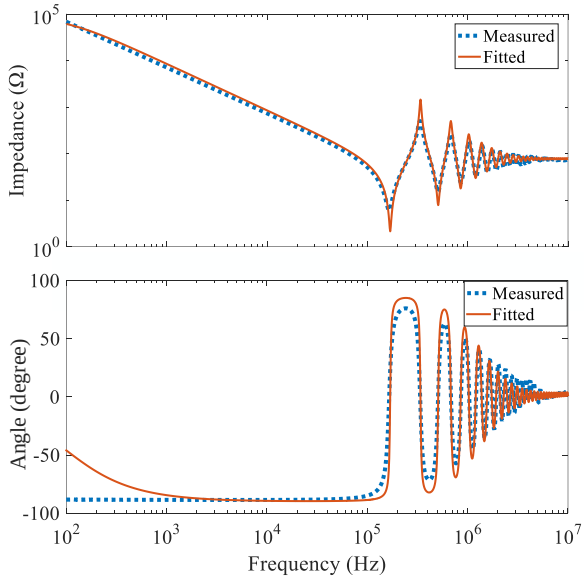

Figure 7. OC impedance of 200m power cable in DM

Preprints (www.preprints.org) | NOT PEER-REVIEWED | Posted: 11 December 2020 doi:10.20944/preprints202012.0286.v1

Based on the per-unit cable model and its parameters shown in Table 3, the model of 200m cable can be constructed with 200 segments, and its high-frequency impedance simulated should be compared with the measured ones to verify its effectiveness. Taking the DM characteristics of 200m cable as example (Figure 6 & Figure 7), apparently, the frequency response based on the proposed model is in good agreement with the measured cable characteristic.

4. Experimental Verification of the DM Overvoltage and CM Current

In order to validate the proposed modeling technique in this paper further and the predicted phenomenon based on simulation, the test platform (Figure 8) has been constructed, including the 750W drive system, 200m cable, and 750W permanent synchronous motor (PMSM). The drive system is made up with the active rectifier and the inverter, where the latter is the key factor in the drive system affecting the DM voltage and CM current, with parameters of 380V DC voltage and 16kHz switching frequency. In addition, the rise time and fall time of IGBT in the inverter are approximately 0.21us and 1.6us respectively, but they are only typical values because the switching time is varying with the load.

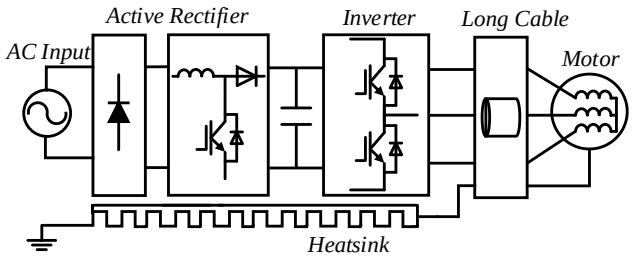

Figure 8. Experimental platform to validate the proposed model

4.1. Inverter and Motor Model

The inverter and motor should also be included to make up the entire long cable system to investigate the problems caused by long cables and high switching speed. The inverter is the voltage source of long cable system, which could be equivalent as a voltage pulse of trapezoidal shape with a low internal impedance, or no internal impedance since it is almost negligible compared with the characteristic impedance of cable.

Similar to the cable modeling, the parameters of motors are also frequency-dependent, including stator magnetizing inductance, stator leaking inductance, wingding turn-to-turn coupling capacitive and etc. There are numerous literatures about the high-frequency model of motors, but all the complex models play a limited role in most overvoltage simulations, thus some simplifications could be adopted. The high-frequency reflection coefficients at the motor terminal is 0.95 for small hp motors, 0.65 for 500 hp motors, indicating that the impedance of motors is much larger than the characteristic impedance of cable in high-frequency region. Therefore, the small hp motors could be equivalent as open circuit, or these could be simplified as RL circuits even for big hp motors.

In general, the cable model is the most important and complex part of the long cable system, and the model of the inverter and motor could be simplified owing to their rather minor influence in most occasions, which will be verified in the following content.

4.2. Overvoltage Analysis

In this section, the simulation and experimental results of line-to-line voltage at the motor side are presented to verify the feasibility of proposed system model, including inverter, long cables and motors. The experimental overvoltage at the motor side will be compared with that of simulation, not only include the proposed cable model but also other cable models available in different simulator programs, like Matlab and Pspice. Figure 9 shows the simulation waveforms of proposed cable model

Preprints (www.preprints.org) | NOT PEER-REVIEWED | Posted: 11 December 2020 doi:10.20944/preprints202012.0286.v1

that are almost superimposed with the experimental counterparts, and the fitting performance of overvoltage could be further improved if the simulated output voltage of the inverter keeps same with that of experiment. There are some typical cable models used here for the comparation with the proposed model, including the PI model of MATLAB and TLOSSY model of Pspice, which are both lack the frequency-dependant characteristics of cable parameters. From Figure 10, the fitting performances of overvoltage are much worse either in magnitude or damping compared with the simulation results of the proposed model. Besides, for the high-frequency model constructed in most paper without considering accuracy of the cable resistance, the damping of simulated overvoltage will be affected. In order to demonstrate such analysis, the cable resistance of the proposed model is decreased to the one fourth of its original value, then the Figure 11 shows that the damping of overvoltage waveform is not enough.

Based on Bewley lattice diagram [20], if the rise time of voltage source is less than twice the propagation time, the overvoltage at the end of cable is twice the dc-bus voltage, which is the maximum overvoltage simultaneously. Whereas, from the overvoltage figure in this paper, it can be observed that the amplitude of overvoltage at motor side is more than two times dc-bus voltage, because the oscillation frequency is so small for very long cables that the remained voltage at the end of cable is still high before the application of next voltage pulse. The overvoltage problem will be more severe if the duty ratio of PWM is bigger, posing a big threat to the motor. Besides, the overvoltage will introduce the huge current spike through parasitic capacitance of cable, which will affect the motor control and the efficiency of the entire system.

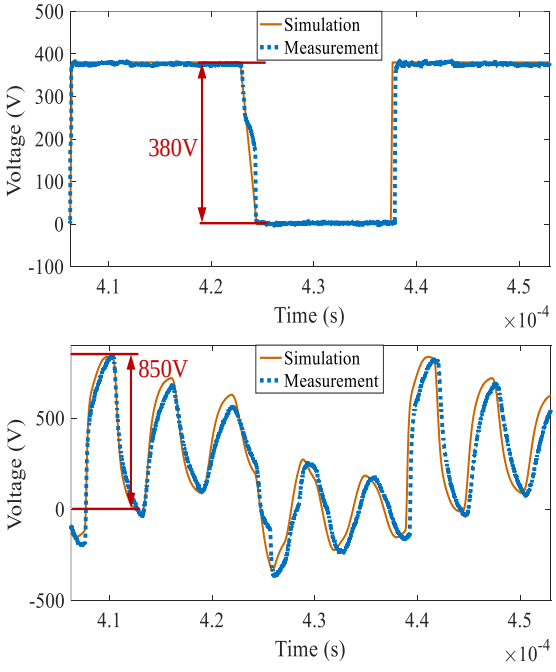

Figure 9. Comparation of the line-to-line voltage at the inverter side (upper curve) and at the motor side (bottom) with the proposed model

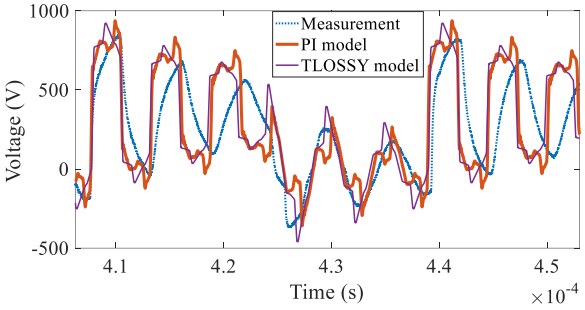

Figure 10. Comparation of the line-to-line overvoltage at the motor side with the PI model and TLOSSY model

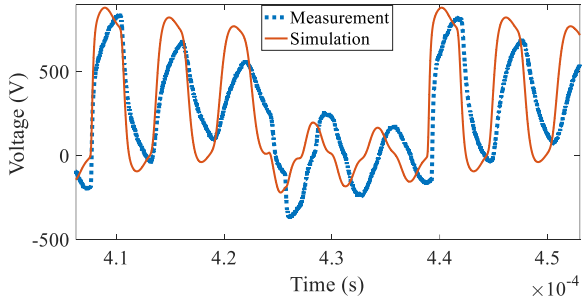

Figure 11. Comparation of the line-to-line overvoltage at the motor side with the model of low cable resistance

4.3. CM Current Analysis

Different with the inverter model of DM equivalent circuit, the CM voltage source should be one third the magnitude of the DM voltage source. The CM current analysis is carried out on the same test platform, and the measured point of CM current is put on the beginning of the long cable to get rid of the effects of the drive system, such as the parasitic capacitance between the inverter and the ground. Compared with the DM simulation, it's hard to keep the high accuracy of CM current

Preprints (www.preprints.org) | NOT PEER-REVIEWED | Posted: 11 December 2020 doi:10.20944/preprints202012.0286.v1

simulation, because of its sensitivity even affected by some trivial factors, like the capacitive coupling of the cable.

If the motor driver is directly connected with the motor through 200m long cables in the test platform, the Ground Fault Circuit Interrupter (GFCI) with 30mA protection threshold will respond owing to the enormous CM current (Figure 12), consisting of high-frequency components though. At the beginning of the experimental CM current, there are some small-current regions caused by the start-up strategy of motor control like the pre-position technique. As it has shown in Figure12, the peak value of CM current is very high, once the motor starts up, the power will be disconnected in the response time of GFCI. For the purpose of getting stable experimental results of the CM current with long cables to verify the simulation of the CM current, the length of test cable needs to be reduced to 20m, whose CM current is not big enough to trip the protection of GFCI. The experimental results of 20m power cable are shown in Figure 13, of which the magnitude, ring frequency and damping of simulation are all close to the simulation results of the proposed model that has better performance than the PI model and TLOSSY model. Therefore, the CM model of the drive system could be used to predict the stable CM current of 200m cable that is not convenient to be measured in the experiment as discussed before, demonstrating the modeling significance to some extent. It's noted that the current threshold of GFCI protection is the rating current flowing to the ground in low frequency range and its protection threshold will be increased if the frequency of ground current is higher. Nevertheless, the suppression the enormous CM current is a big challenge in the long cable system.

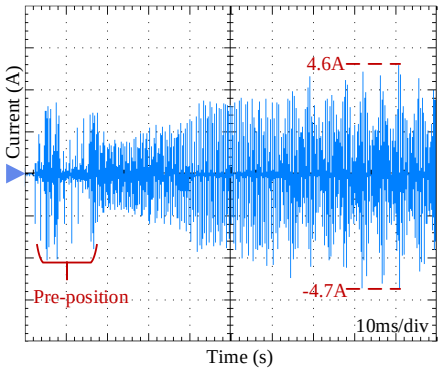

Figure 12. Measured CM current of 200m cable

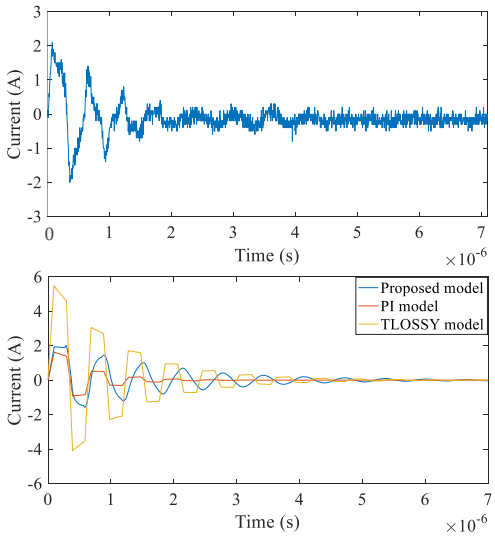

Figure 13. CM current comparison of measurement (upper curve) and simulation (bottom) for 20m cable

Preprints (www.preprints.org) | NOT PEER-REVIEWED | Posted: 11 December 2020 doi:10.20944/preprints202012.0286.v1

5. Filter Design

The filter design can be divided into two parts, the DM filter to suppress the overvoltage at the motor terminal and the spike current at the inverter side, and CM filter to mitigate the CM current. The filters discussed here are connected to the inverter side rather than the motor side, since it's usually inconvenient to connect the filters to the motor directly.

In term of the problems in the long cable drive system, there are some similar requirements should be satisfied after inserting filters. Aiming to the drive system connected with the PMSM through 200m cables here, there are two requirements should be met: 1) the overvoltage at motor side should be normally less than 20% of DC voltage to guarantee the insulation of motors and cables, 2) CM current should be reduced to the value that the GFCI doesn't respond at least.

5.1. DM filter design

Output line inductor is the simplest solution to the DM overvoltage problem, but it's bulky and has high cost. Instead, RLC and LR dv/dt filter at the inverter side have aroused some attention, both of which the resistance R is equal to the characteristic impedance of cable, which will produce power dissipation, as one of distinct disadvantages when filters are applied in the small power drive system. Therefore, a new filter, LC filter with weak damping, is proposed in this paper to decrease losses but maintain good filtering performance. It should be emphasized that the design mechanism of the proposed DM filter (Figure 15) is different with that of the RLC filter, though their topologies are similar.

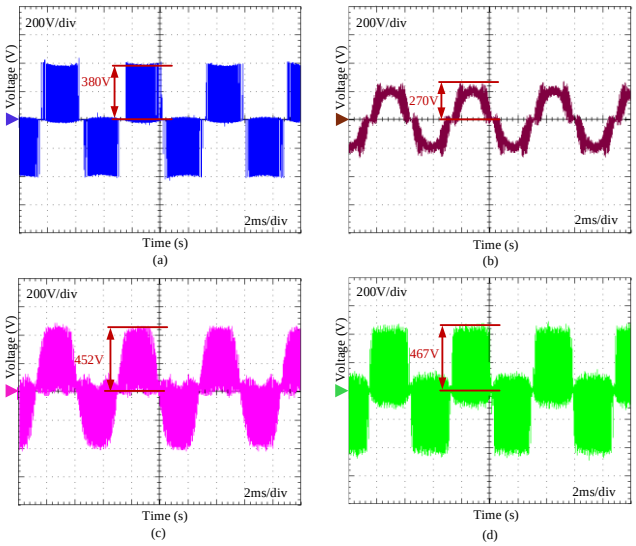

Figure 14. Output voltage of inverter (a) and terminal voltage at motor side with the proposed DM filter (b), RLC filter (c), LR filter (d)

Table 4. Comparation between proposed filter and conventional filters

	Proposed Filter	**RLC Filter**	**LR Filter**
Number of Components	9	9	6
Volume	small	big	small
Overvoltage	none	19%	23%
Filter losses	20W	290W	135W

Preprints (www.preprints.org) | NOT PEER-REVIEWED | Posted: 11 December 2020 doi:10.20944/preprints202012.0286.v1

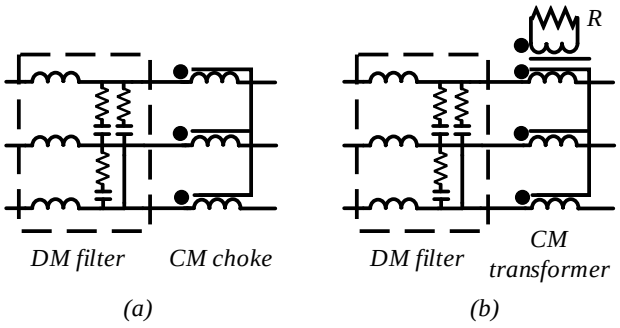

Figure 15. Proposed filter network with CM choke (a) and filter network with CM transformer (b)

As for LC filter, its natural oscillation frequency should be far from the main frequency of the drive system, like the switching frequency of the inverter (f_{PWM}) and motor running frequency (f_{motor}). Furthermore, in order to prevent the oscillation of LC filter due to the disturbing from the surrounding environment, weak damping is inserted to make up the proposed filter. In other words, the proposed filter is essentially a sine-wave filter, which seems to be unnecessary and overdesigned than conventional RLC and LR dv/dt filter. However, under the situation where the cable is very long and overvoltage ratio should be low like the drive system here, the required natural oscillation frequency of filter will be close to or even lower than the switching frequency regardless of any sorts of filters, then the merit of the proposed filter is much more distinct than the conventional RLC filter and LR filter, not only in the volume but also the losses. For the RLC filter and proposed filter with the same inductance and capacitor, the former is worse in the ability of suppressing high-frequency harmonic, which is the reason why the output voltage of the RLC filter is still PWM rather than the sinusoidal waveform like the output voltage of LC filter when the natural oscillation frequency of filter isn't much lower than switching frequency of inverter. The parameters of proposed filter can be determined by (15~18), derived from the overvoltage ratio (ξ), the natural oscillation frequency (f_c) of filter and damping ratio of filter (ζ), where tr represents the required rise time of inverter and Γ_L stands for the load reflection efficient. In other words, (15)(16) is intended to make the system satisfy the voltage requirement of motors, and (17)(18) is used to guarantee the robustness and stability of filter, particularly to avoid oscillation of the filter.

$$\frac{2l}{vt_r}(\Gamma_L+1)-1=\xi \tag{15}$$

$$f_c=\frac{1}{2\pi\sqrt{LC}}<\frac{1}{\pi t_r} \tag{16}$$

$$10\,f_{Motor}<f_c=\frac{1}{2\pi\sqrt{LC}}<\frac{1}{2}\,f_{PWM} \tag{17}$$

$$\frac{1}{20}<\zeta=\frac{R}{2}\sqrt{\frac{C}{L}}<\frac{1}{10} \tag{18}$$

According to the design criteria shown above, the parameters of proposed DM filter, designed for the drive system of test platform, have been determined as

$$L_{f\_DM}=427.5uH,\ C_{f\_DM}=0.44\mu F,\ R_{f\_DM}=3.2\Omega \tag{19}$$

Furthermore, the filter parameters of the DM equivalent circuit need to be transferred to the per phase parameters, and the relationship of those parameters in the proposed filter is shown as

$$L_{f\_ph}=\frac{2}{3}L_{f\_DM},\ C_{f\_ph}=\frac{1}{2}C_{f\_DM},R_{f\_ph}=\frac{2}{3}R_{f\_DM} \tag{20}$$

Preprints (www.preprints.org) | NOT PEER-REVIEWED | Posted: 11 December 2020 doi:10.20944/preprints202012.0286.v1

After inserting the proposed DM filter, the voltage at motor side is sinusoidal which is apparently better than the output waveform of RLC filter using same inductance and capacitance, shown in Figure 14. In Table 4, there is a comparison among the proposed filter (L_{f_ph}=285μH, C_{f_ph}=0.22μF, R_{f_ph}=2Ω), RLC filter (L_{f_ph}=285μH, C_{f_ph}=0.22μF, R_{f_ph}=50Ω), and LR filter (L_{f_ph}=285μH, R_{f_ph}=50Ω), which shows the advantage of proposed filter at the aspect of volume, efficiency and suppressing ability of overvoltage. In addition, the high-frequency losses of cables and motors are also eliminated if implementing the proposed filter, because the output voltage of proposed filter is sinusoidal. In general, the proposed filter has high efficiency, smaller volume, and lower overvoltage.

5.2. CM Filter Design

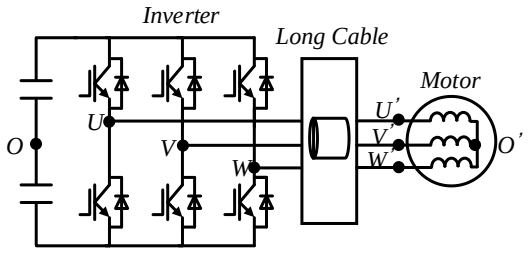

Figure 16. Simplified drive system used to analyze the CM noise

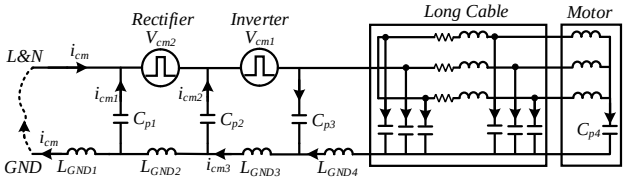

Figure 17. Equivalent CM path of the drive system

The sources of the CM voltage in the entire drive system are rectifier and inverter, and the latter plays a main role. For the convenience of analysis, the modulation of inverter is simplified as the SPWM and the midpoint of DC side is selected as reference potential point, shown in the Figure 16. Then, the common mode voltage (V_{cm1}) at the inverter side can be derived as follows:

$$V_{iO} = S_i \frac{U_{dc}}{2} + (1 - S_i)(-\frac{U_{dc}}{2}) = (2S_i - 1)\frac{U_{dc}}{2} \quad (i = U, V, W) \tag{21}$$

$$V_{cm1} = \frac{V_{UO} + V_{VO} + V_{WO}}{3} = \frac{U_{dc}}{6} \sum_{i=U,V,W} (2S_i - 1) \tag{22}$$

Where S_i is the switching function, if the upper switch of i-phase is on, the function value is 1, otherwise it's 0. Considering the overvoltage ratio (n) at the motor side with long cables and assuming the voltage applied on the long cables is symmetrical, the CM voltage at motor side can be approximately expressed as:

$$V'_{cm1} = \frac{V_{U'O} + V_{V'O} + V_{W'O}}{3} = \frac{nU_{dc}}{6} \sum_{i=U,V,W} (2S_i - 1) \tag{23}$$

In fact, the midpoint (O) voltage of dc-bus side is not equal to the ground (N), and the value of difference (V_{ON}) depends on the topology of rectifier, which is actually a CM voltage source caused by the rectifier.

$$V_{cm2} = V_{ON} \tag{24}$$

For the uncontrolled rectifier or the single active rectifier used here, whose CM source voltage is mainly made up of low frequency components, their high-frequency CM noise is much smaller than that of inverter. In general, the nonlinear components are the CM source, which could be regarded as the voltage source in the CM equivalent circuit, as shown in Figure 17. In the CM equivalent circuit,

Preprints (www.preprints.org) | NOT PEER-REVIEWED | Posted: 11 December 2020 doi:10.20944/preprints202012.0286.v1

C_P denotes the parasitic capacitance including the rectifier, inverter and motor to ground, and L_{GND} represents the ground inductance of ground path. Besides, the arrows of current don't imply the actual flowing direction, and the CM current flowing out the drive system can be expressed as:

$$i_{cm} = i_{cm3} - (i_{cm1} + i_{cm2}) \tag{25}$$

Therefore, in order to decrease the value of CM current (i_{cm}) flowing out the drive system, the value of i_{cm1} and i_{cm2} should be increased, like through paralleling capacitance before the CM source, or adding CM inductance at the AC side, and the value of i_{cm3} should be decreased, like through adding the CM filter after the inverter. As for the CM filter at the inverter side, if using the CM choke, the saturation current should be high enough due to the large CM current caused by long cables. The inductance of CM choke designed in the test platform is 10mH, with the rated saturation current of 0.2A. However, the CM transformer (Figure 15) is an alternative choice to decrease the volume of the CM filter, which requires lower saturation current almost without adding cost. Compared with CM choke, the CM transformer introduce a damping resistor to mitigate the oscillation of CM current and decrease its peak value. The theorical design of damping resistance has been clarified in [21], which could be verified ahead of experiment, based on the constructed model of the drive system. After inserting the CM filter, the CM current is extremely small, thus the dissipation on the damping resistor is very small and the area of secondary winding could be thin, contributing to the priority of the CM transformer combined with a smaller magnetic core compared with the CM choke. In the experiment, a CM transformer with 4.3mH inductance and 2500 Ω has been inserted and corresponding CM current waveform has been shown in Figure 18, where the CM current has been decreased a lot compared with that in Figure 12. In addition, the loss of CM filter is about 6.25W, then the total loss of proposed filter in Figure 15(b) is 26.25W.

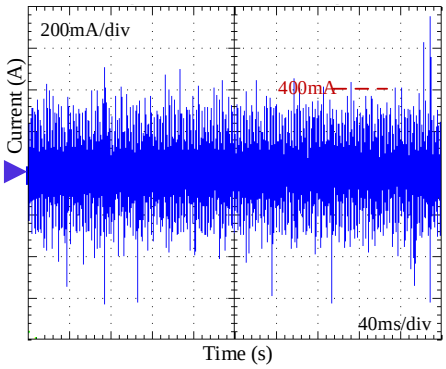

Figure 18. CM current of 200m cable after inserting the CM transformer

6. Conclusion

This paper has analyzed the importance of high-frequency resistance of cable that is an easily overlooked factor in the process of cable modeling. Then, both high-frequency models are proposed to accurately describe the characteristics of power cables in a wide frequency range, but the ladder model requires enormous calculation and it takes more time to simulate the model. The model parameters are identified through the DM and CM impedance characteristics measured by the impedance analyzer, with analytical design equations given in this paper. Combined with the simplified inverter model and motor model, the model of the whole drive system has been constructed to predict the DM overvoltage and CM current. The simulation results are in good agreement with the experimental waveform, indicating the effectiveness of the proposed model.

Considering high losses of conventional DM filters, a new filter at the motor side is proposed to mitigate the DM overvoltage. The new DM filter has been validated with experiments and compared with two sorts of conventional DM filters, showing the advantage of the proposed DM filter in the aspects of the volume, losses and suppressing ability. For the suppression of CM current, CM choke

and CM transformer are adopted in this paper, either of which forms the entire filter network with the proposed DM filter. The filter networks are more effective in the small power drive system with long cables and motors that requires a strict working voltage.

Author Contributions

Conceptualization, W.W.; methodology, L.W.; software. L.W.; validation, Y.Z. and M.S.A.; formal analysis, L.W.; investigation, G.C. and J.M.G.; data curation, L.W.; writing—original draft preparation, L.W.; writing—review and editing, G.C. and J.M.G.; supervision, J.C.V. and J.M.G.; funding acquisition, J.M.G. All authors have read and agreed to the published version of the manuscript.

Funding

This work was supported by VILLUM FONDEN under the VILLUM Investigator Grant (No. 25920): Center for Research on Microgrids (CROM); www.crom.et.aau.dk

Conflicts of Interest

The authors declare no conflict of interest.

References

1. Zhang, Z.; Wang, F.; Tolbert, L.M.; Blalock, B.J.; Costinett, D. Evaluation of switching performance of SiC devices in PWM inverter fed induction motor drives. *2014 IEEE Energy Convers. Congr. Expo. ECCE 2014* **2014**, *30*, 1597–1604.
2. Smochek, M.; Pollice, A.F.; Rastogi, M.; Harshman, M. Long cable applications from a medium-voltage drives perspective. *IEEE Trans. Ind. Appl.* **2016**, *52*, 645–652.
3. De Paula, V.C.; De Paula, H. Employing DC transmission in long distance AC motor drives: Analysis of the copper economy and power losses reduction in mining facilities. In Proceedings of the IEEE Industry Application Society - 51st Annual Meeting, IAS 2015, Conference Record; 2015.
4. Song, Y.; Ebrahimzadeh, E.; Blaabjerg, F. Analysis of High-Frequency Resonance in DFIG-Based Offshore Wind Farm via Long Transmission Cable. *IEEE Trans. Energy Convers.* **2018**, *33*, 1036–1046.
5. Jiang, Y.; Wu, W.; He, Y.; Chung, H.S.H.; Blaabjerg, F. New Passive Filter Design Method for Overvoltage Suppression and Bearing Currents Mitigation in a Long Cable Based PWM Inverter-Fed Motor Drive System. *IEEE Trans. Power Electron.* **2017**, *32*, 7882–7893.
6. Mirafzal, B.; Skibinski, G.L.; Tallam, R.M. Determination of parameters in the universal induction motor model. *IEEE Trans. Ind. Appl.* **2009**.
7. Magdun, O.; Binder, A.; Purcarea, C.; Rocks, A. High-frequency induction machine models for calculation and prediction of common mode stator ground currents in electric drive systems. *2009 13th Eur. Conf. Power Electron. Appl. EPE '09* **2009**.
8. Pulsinelli, F.; Solero, L.; Chiola, D.; Sobe, K.; Brucchi, F. Overvoltages at Motor Terminals in SiC Electric Drives. *SPEEDAM 2018 - Proc. Int. Symp. Power Electron. Electr. Drives, Autom. Motion* **2018**, 513–518.
9. Stevanovic, I.; Wunsch, B.; Skibin, S. Behavioral high-frequency modeling of electrical motors. *Conf. Proc. - IEEE Appl. Power Electron. Conf. Expo. - APEC* **2013**, *2*, 2547–2550.
10. Schinkel, M.; Weber, S.; Guttowski, S.; John, W.; Reichl, H. Efficient HF modeling and model parameterization of induction machines for time and frequency domain simulations. *Conf. Proc. - IEEE Appl. Power Electron. Conf. Expo. - APEC* **2006**, *2006*, 1181–1186.
11. Moreira, F.A.; Martí, J.R.; Zanetta, L.C. Latency techniques applied to the transient simulation of

 doi:10.20944/preprints202012.0286.v1

transmission lines using the Z-Line Model. *2006 IEEE PES Transm. Distrib. Conf. Expo. Lat. Am. TDC'06* **2006**, 1–6.

12. Boglietti, A.; Carpaneto, E. Induction motor high frequency model. In Proceedings of the Conference Record - IAS Annual Meeting (IEEE Industry Applications Society); 1999.
13. De Paula, H.; de Andrade, D.A.; Chaves, M.L.R.; Domingos, J.L.; de Freitas, M.A.A. Methodology for cable modeling and simulation for high-frequency phenomena studies in PWM motor drives. *IEEE Trans. Power Electron.* **2008**, *23*, 744–752.
14. Skibinski, G.; Leggate, D.; Kerkman, R. Cable characteristics and their influence on motor over-voltages. *Conf. Proc. - IEEE Appl. Power Electron. Conf. Expo. - APEC* **1997**, *1*, 114–121.
15. Skibinski, G.; Tallam, R.; Reese, R.; Buchholz, B.; Lukaszewski, R. Common mode and differential mode analysis of three phase cables for PWM AC drives. *Conf. Rec. - IAS Annu. Meet. (IEEE Ind. Appl. Soc.* **2006**, *2*, 880–888.
16. Weber, S.P.; Hoene, E.; Guttowski, S.; John, W.; Reichl, H. Modeling induction machines for EMC-analysis. *PESC Rec. - IEEE Annu. Power Electron. Spec. Conf.* **2004**, *1*, 94–98.
17. Akagi, H.; Matsumura, I. Overvoltage mitigation of inverter-driven motors with long cables of different lengths. *IEEE Trans. Ind. Appl.* **2011**, *47*, 1741-1748.
18. Rendusara, D.A.; Enjeti, P.N. An improved inverter output filter configuration reduces common and differential modes dv/dt at the motor terminals in PWM drive systems. *IEEE Trans. Power Electron.* **1998**, *13*, 1135–1143.
19. Moreira, A.F.; Lipo, T.A.; Venkataramanan, G.; Bernet, S. High-frequency modeling for cable and induction motor overvoltage studies in long cable drives. *IEEE Trans. Ind. Appl.* **2002**, *38*, 1297–1306.
20. Tallam, R.M.; Member, S.; Skibinski, G.L.; Shudarek, T.A.; Lukaszewski, R.A.; Member, S. Integrated Differential-Mode and Common-Mode Filter to Mitigate the Effects of Long Motor Leads on AC Drives. **2011**, *47*, 2075–2083.
21. Ogasawara, S. Modeling and damping of high-frequency leakage currents in PWM inverter-fed AC motor drive systems. *IEEE Trans. Ind. Appl.* **1996**, *32*, 1105–1114.
22. Wang, L.; Ho, C.N.M.; Canales, F.; Jatskevich, J. High-frequency modeling of the long-cable-fed induction motor drive system using TLM approach for predicting overvoltage transients. *IEEE Trans. Power Electron.* **2010**, *25*, 2653–2664.